treatment, indicating internal localization of the same. This finding explains the Cu(II)-sensitivity in the strain CS2.

In conclusion, we can say that Cu(II) is toxic to the system and induces several ultrastructural alterations. Being an essential ion, its entry into the cell cannot be prevented. The resistant cells must therefore encode some mechanism to avoid the toxic action. *Candida guilliermondii* strain DS31 has adapted a strategy to accumulate Cu(II) extracellularly so that it could survive under high levels of this metal.

1. Brown, N. L., Rouch, D. A. and Lee, B. T. O., *Plasmid*, 1992, **27**, 41–51.
2. Cervantes, C. and Gutierrez-Corona, F., *FEMS Microbiol. Rev.*, 1994, **14**, 121–138.
3. Silver, S., *Gene*, 1996, **179**, 9–19.
4. Ge, Z. and Taylor, D. E., *FEMS Microbiol. Lett.*, 1996, **145**, 181–188.
5. Odermatt, A., Suter, H., Krapf, R. and Solioz, M., *Ann. N.Y. Acad. Sci.*, 1992, **671**, 484–486.
6. Rouch, D., Camakaris, J. and Lee, B. T. O., in *Metal–Ion Homeostasis: Molecular Biology and Chemistry* (eds Hamer, D. H. and Winge, D. R.), Alan R. Liss, Inc., New York, 1989, pp. 45–105.
7. Cha, J. S. and Cooksey, D. A., *Proc. Natl. Acad. Sci. USA*, 1991, **88**, 8915–8919.
8. Gilotra, U. and Srivastava, S., *Curr. Microbiol.*, 1997, **34**, 378–381.
9. Bitton, G. and Freihofer, V., *Microb. Ecol.*, 1970, **4**, 119–125.
10. Kneer, R., Kutchan, T. M., Hochberger, A. and Zenk, M. H., *Arch. Microbiol.*, 1992, **157**, 305–310.
11. Saxena, D. and Srivastava, S., *World J. Microbiol. Biotechnol.*, 1998, **14**, in press.
12. Mergeay, M., Nies, D., Schlegel, H. G., Gerits, J., Charles, P. and Gijsegem, F. V., *J. Bacteriol.*, 1985, **162**, 328–334.
13. Venkateswerlu, G., Yoder, M. J. and Stotzky, G., *Appl. Microbiol. Biotechnol.*, 1989, **31**, 204–210.
14. Cabral, J. P. S., *J. Gen. Microbiol.*, 1990, **136**, 2481–2487.
15. Sigee, D. C. and AL-Rabaee, R. H., *Protoplasma*, 1986, **130**, 171–185.
16. Vaituzis, Z., Nelson, J. D., Jr., Wan, L. W. and Cotwell, R. R., *Appl. Microbiol.*, 1975, **29**, 275–286.
17. Bhagat, R. and Srivastava, S., *J. Gen. Appl. Microbiol.*, 1994, **40**, 265–270.
18. Gelmi, M., Apostoli, P., Cabibbo, E., Porru, S., Alessio, L. and Turano, A., *Curr. Microbiol.*, 1994, **29**, 335–341.
19. Ramamoorthy, S. and Kushner, D. J., *Microb. Ecol.*, 1975, **2**, 162–176.
20. Tohoyama, H., Inouhe, M., Joho, M. and Murayama, T., *J. Indian Microbiol.*, 1995, **14**, 126–131.

ACKNOWLEDGEMENT. This work was supported by assistance from UGC, India, to DS.

Received 24 August 1998; revised accepted 9 November 1998

The meandering Indus channels: Study in a small area by the multibeam swath bathymetry system – Hydrosweep

V. N. Kodagali* and Pratima Jauhari

Geological Oceanography Division, National Institute of Oceanography, Dona Paula, Goa 403 004, India

The discharge of sediments by the river Indus has accumulated into a 2500 m thick pile, forming one of the largest deep sea fans in the world. Though there are many reports on channels in different regions of the fan, we report for the first time the presence of distinct channels far from the mouth of the fan. A multibeam seafloor mapping system, Hydrosweep has been used to trace the channels and determine related physical parameters. The channels are largely comparable in size and shape to some of the world's largest fluvial systems.

LITHOGENIC influx due to erosion of the Himalaya has resulted in formation of the Bengal and the Indus Fans[1]. Both have formed predominantly due to turbidites originating from the mouths of the Indus and the Ganges–Brahmaputra river systems[2]. Most of the turbidity flows have taken place during the Pleistocene and earlier times of lowered sea level, and are thought to have been inactive during the Holocene[3].

In the past the Indus river discharged 200 cubic km of water annually, and carried to the head of the Arabian Sea some 450 million tonnes of suspended sediment[4]. Today, the sediment discharge has been reduced to 45 million tonnes due to the construction of dams and barrages. The piling of sediments has created the Indus cone, a 2500 m thick pile of loose sediments on the floor of the Arabian Sea, 1500 to 2500 km away from the mouth of the river. Some of the sediments settled immediately giving rise to the Indus delta. The rest have been carried to deeper areas of the Arabian Sea by turbidity currents as a dense sediment suspension through the Indus Canyon[4].

The bathymetry and internal structure of these fans, deltas and cones have been studied by numerous investigators[5,6]. Sedimentation and mechanism of sediment transport in the entire fan has also been studied[7,8]. The available data on bathymetry, shallow acoustic character of the sea floor, seismic stratigraphy, internal structure and sediment distribution of the entire Indus fan have been compiled[9]. However, the area undertaken for the present study has not been studied.

The 'GLORIA' side scan sonar and seabeam swath bathymetry system allows individual channels to be

*For correspondence. (e-mail: kodagali@csnio.ren.nic.in)

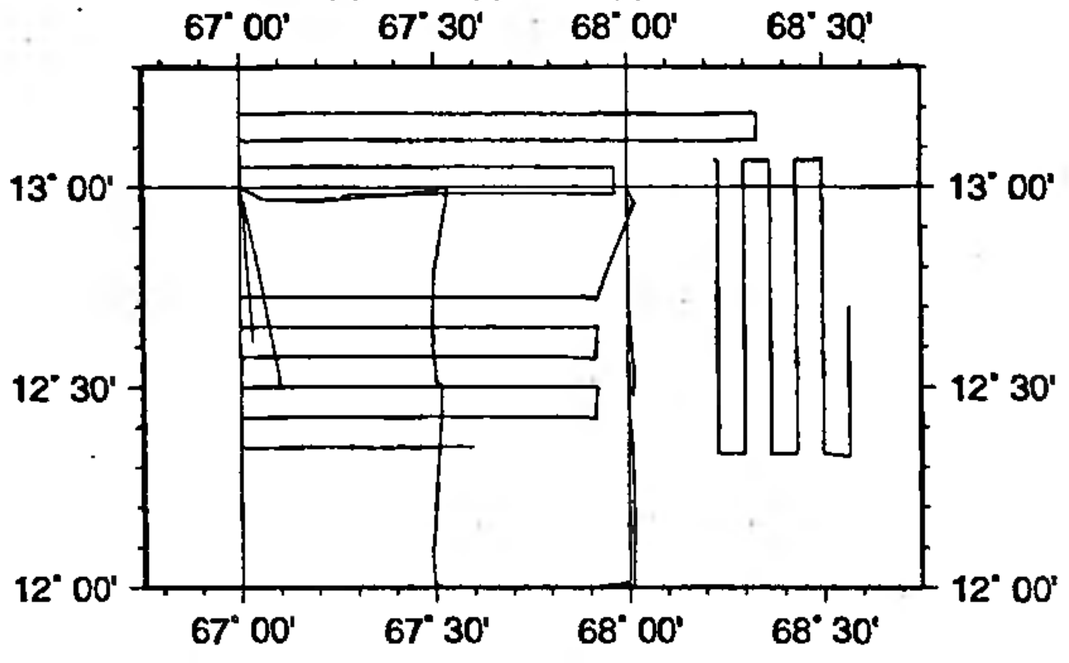

Figure 1. Location map and the Hydrosweep survey tracks in the area.

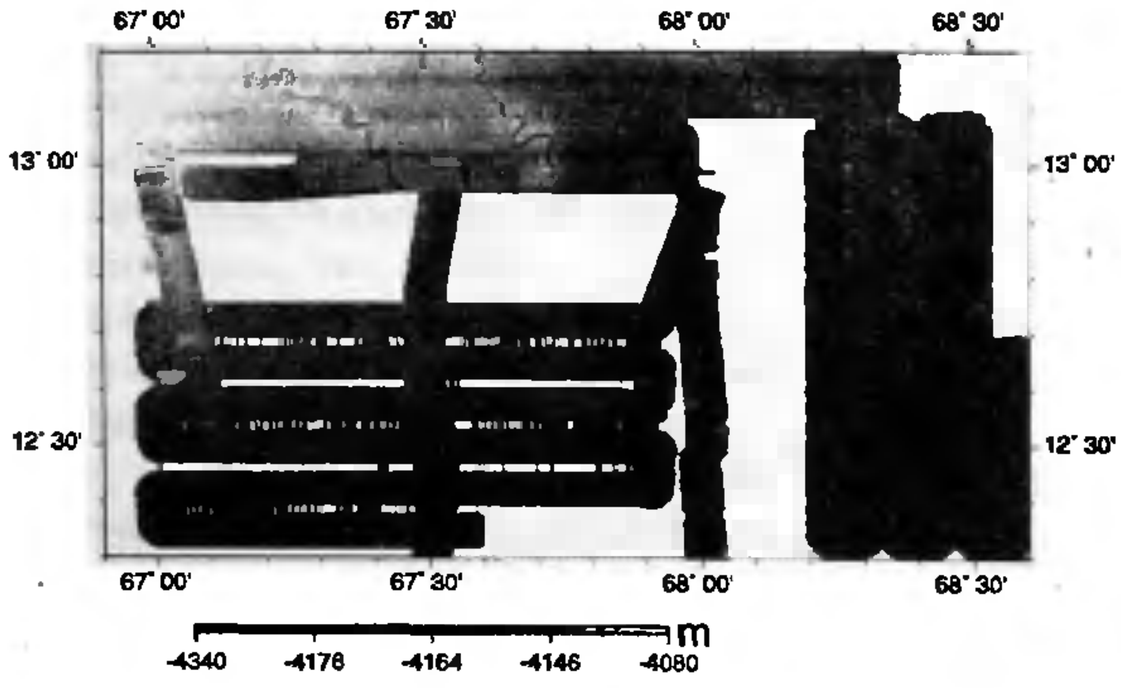

Figure 2. Grey shaded depth contour map showing the meandering channels.

traced over long distances, and to map them accurately[10–12]. The geometry of submarine channels measured from the GLORIA side scan sonar data have been studied for 16 different submarine fans[13]. But study of individual channels has not been undertaken for the Indus channels. Sporadic attempts have been made to study the meandering Indus channels existing at deeper water depths. Here we study these meandering channels.

A multidisciplinary cruise was undertaken in 1993 on ORV Sagar-Kanya covering an area between 12°00' and 13°20'N lat. and 66°30' to 69°E long. Multibeam swath bathymetry system, Hydrosweep, was run in parellel tracks (Figure 1). The Hydrosweep works at 15.5 kHz using 59 preformed beams (for technical details of the system, see ref. 14). The cruise tracks were spaced at 4 nm. Though this provided good coverage of the seafloor, the entire area could not be covered, resulting in areas with no data as seen in Figure 2. The post processing of Hydrosweep data shows five distinct meandering channels as far up to 12°18'N lat. between 67° and 68°30'E long. at a water depth of 4,200 m (Figure 2). One of the meandering channels appears to be in the state of getting modified into an oxbow lake. The Hydrosweep was used to measure parameters such as the channel width, channel meander wavelength, radius of curvature, amplitude and turtuosity (ratio between meander length and channel width).

The data revealed presence of five distinct channels at 4,200 m depth. One of the channels at 67°15'E appears to have a double wall side. Figure 2 shows grey shaded depth contour in the study area. The water depths over the entire fan varies from 1,400 to 1,600 m at the foot of the continental slope to greater than 4,500 m at the Carlsberg ridge[9]. The water depth in our area of study is about 4,200 m. The normally prepared depth contour maps (25 m contour interval) did not show these channels properly. Hence, a grey shaded depth contour map (Figure 2) was prepared. We highlight these channels on the sketch given in Figure 3. The slope angle contour map (gradient of the field) is shown in Figure 4. The channels show steep angles at 15°–30°. Other parameters obtained using the Hydrosweep are tabulated in Table 1. The sinuosity, meander patterns and associated morphological features of these channels are quite similar to meander patterns and associated flood plain features of large fluvial systems on land, such as those of the lower Mississippi river[13].

Our study shows that the channel distributaries extend as far as 12°N lat. (Figure 2). The channels are very distinct, meandering, and continue further down. The canyon floors of the Indus are erosional in their proximal part but become channel–levee systems with aggradational

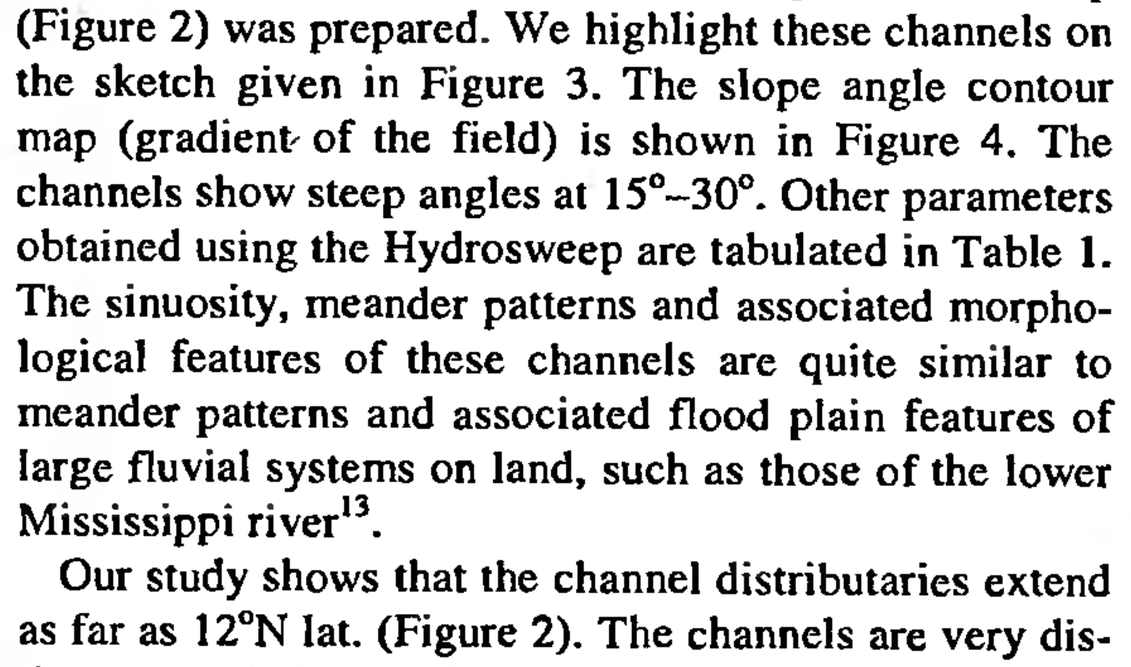

Figure 3. Traced paths of the deciphered channels.

Table 1. Channel parameters obtained using the sea floor mapping system: Hydrosweep

Channel	No. of bends	Depth	Meander length (m) *X*	Channel width (m) *Y*	Amplitude	Radius of curvature	Turtuosity ratio *X/Y*
1	10	25, 30	4650, 9000	854, 597	3400	1200	5.4, 15
2	4	25	10200	940	5500	1200	10.85
3	3	28	10200	1100	3400	1750	9.27
4	7	30	5500	1195	2820	900	5.05
5	4	20	3840,5100	854	3400	1700	9.5, 5.97

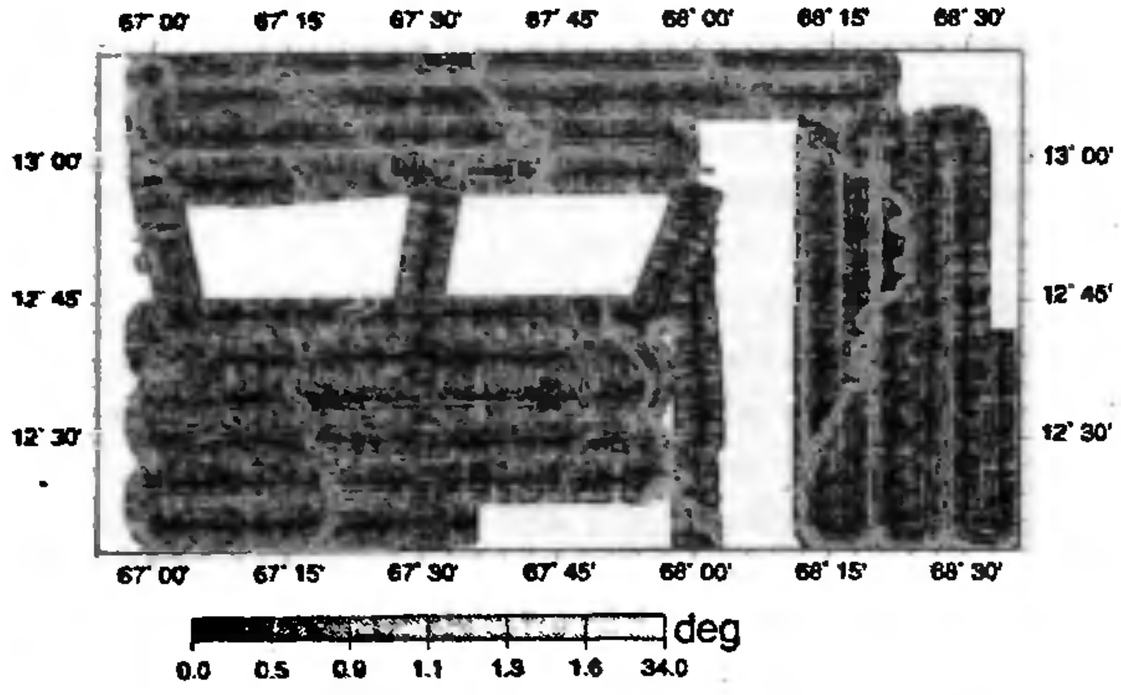

Figure 4. Slope angle contour (contour interval 3 degrees) of the area.

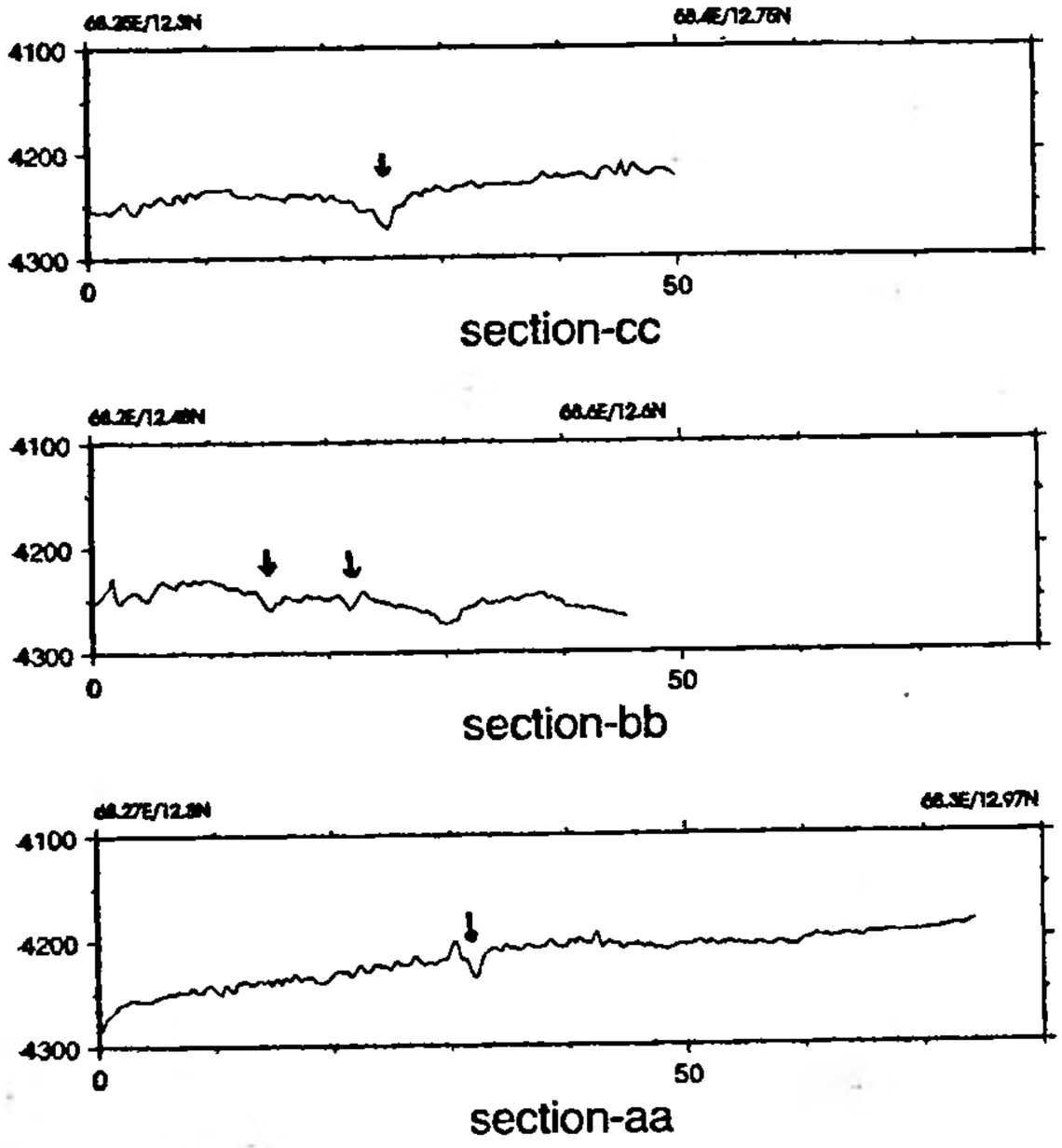

Figure 5. Cross-section profiles across the channels. Arrows indicate location of the channels. Beginning and end of profiles are indicated on top of each profile.

channel floors further down the fan[7]. Several large channel–levee systems that emanate from near the mouth of each Canyon complex are equivalent in size and location to those in the Amazon fan[13]. Together they form first-order channel–levee complexes. The large channel–levee systems are enormous sediment bodies, up to 500 km long and 80 km wide with a maximum levee thickness of 1100 m. There is a progressive decrease in their size down the fan. The Indus fan has been divided into upper, middle and lower fan regions. Though there are many reports on distinct channels in different regions of the fan, our study reports presence of the channels far from the mouth of the fan. In fact, it appears that the channels extend farther south. The morphology of the channels as well as the valley slope are influenced by the type of the sediment transported[15]. In addition, factors such as flow type, seafloor topography, and tectonic events may also affect the channel course. The channel sinuosity increases with increase in the slope in such a way that it maintains an optimum channel slope suitable to accommodate the volume of flow and sediment load in the channel[16]. Study of sediment samples from the area, preferably using long cores, is needed to understand the mechanism of transport of sediments in the basin.

Figure 5 shows the cross-section of the channel profiles in the area studied. The arrows on the profile indicate locations of channels. The eastern-most channel marked as 1 has highest number of bends (10) as compared to channel 3 which has only 3 bends. The average depth of the channels is 26 m, the highest recorded depth for channel 4 and 1 is 30 m, whereas channel 5 is the shallowest with 20 m depth. The meander length of the channels in the area varies from 3,840 m to 10,200 m whereas the channel width varies from 597 to 1,195 m. The ratio between meander length and the channel width (turtuosity) ranges from 5.0 to 15.0 in the area (Table 1).

It is interesting to note that though the study area is almost horizontal, the channels are not linear. They seem to bend towards the east. There is no evidence that this is controlled by topographic variation. Hence, some tectonic control is likely.

1. Kolla, V. and Kidd, R. R., in *The Ocean Basins and Margins* (eds Nairn, A. E. M. and Stehli, F. G.), Plenum Press, New York, 1982, pp. 1–50.
2. Ramaswamy, V., in *Monsoon Biogeochemistry*, SCOPE/UNEP Sonderband, 1993, 97–117.
3. Kolla, V. and McCurda, Jr. D. B., in *Sea Level Changes – An Integrated Approach*, SEPM special publication, 1988, 42, 381–392.

4. Nair, R. R., *New Sci.*, 1984, 16Feb, 41–43.
5. Coumes, F. and Kolla, V., in *Marine Geology and Oceanography of Arabian Sea and Coastal Pakistan* (eds Haq, B. U. and Milliman, J. D.), Van Nostrand Reinhold, New York, 1984, pp. 101–110.
6. McHargue, T. R. and Webb, J. E.,. *Bull. Am. Ann. Petrol. Geol.*, 1986, **70**, 161–180.
7. Naini, B. R. and Kolla, V., *Mar. Geol.*, 1982, **47**, 181–195.
8. Kolla, V. and Coumes, F., *Geo-Mar. Lett.*, 1984, **3**, 133–138.
9. Kolla, V. and Coumes, F., *Am. Assoc. Petrol. Geol.*, 1987, **71**, 650–677.
10. Garison, L. E., Kenyon, N. H. and Bouma, A. H., *Geo-Mar. Lett.*, 1982, **2**, 31–39.
11. Bellaiche, G. *et al.*, *Acad. des Sci., Compt. Rend.*, 1983, **296**, 579–583.
12. Kenyon, N. H., Amir, A. and Cramp, A., in *Atlas of Deep Water Environments: Architectural Style in Turbidite Systems* (eds Pickering, K. T., Hiscott, R. N., Kenyon, N. H., Ricci Lucci, F. and Smith, R. D. A.), Chapman and Hall, London, 1995.
13. Damuth, J. E., Kolla, V., Flood R. D., Kowsmann, R. O., Monteiro, M. C., Gorini, M. A., Palma, J. J. C. and Belderson, R. H., *Geology*, 1983, **11**, 94–98.
14. Gutbertlet, M. and Schenke, H. W., *Mar. Geodesy*, 1989, **33**, 1–24.
15. Clark, J. D., Kenyon, N. H. and Pickering, K. T., *Geology*, 1992, **20**, 633–636.
16. Chumm, S. A. and Khan, H. R., *Bull. Geol. Soc. Am.*, 1972, **74**, 1089–1100.

ACKNOWLEDGEMENTS. We thank Mr R. R. Nair for constructive suggestions and Dr Satish Shetye for reviewing the article. NIO contribution no. 2607.

Received 21 April 1998; revised accepted 23 October 1998

Using global positioning system for orthometric height determination for gravity surveys in Ladakh Himalaya

Paramesh Banerjee and Satyaprakash

Wadia Institute of Himalayan Geology, 33 Gen. Mahadeo Singh Road, Dehra Dun 248 001, India

Though GPS can be used for precise 3-D positioning, the height thus measured is spheroidal which needs to be converted to the orthometric height for any practical use. This requires knowledge of the geoid undulation that can either be measured using GPS/levelling technique, or can be modelled from gravity data. We carried out extensive field measurements along a 100 km long transect in Ladakh Himalaya to study the viability of using the GPS for orthometric height determinations required for gravity surveys. Geoid of the study area was also predicted using global gravity models, e.g. OSU91 and EGM96. It is seen that even on high and difficult terrain like that of the Himalaya, GPS can be used for orthometric height determination with an absolute accuracy of 1–2 m.

ACCURATE three-dimensional relative positioning is now possible using GPS[1–4]. A 100 km long baseline can be measured with a repeatability of only few mm. Exhaustive field experiments were conducted by USGS[2]. The RMS residual about the best fit line of 233 km long baseline were 0.03, 0.05 and 0.18 ppm for the north, east and vertical components. The difference between GPS results and Geodilite (a high precision LASER distance measurement) was always less than 1 s.d. A GPS data comparison between VLBI and GPS measurements over common baseline gave a difference of 0.05 ppm, close to 1 s.d. of GPS data.

The initial accuracy barrier like 'anti-spoofing' and 'selective availability' (S/A) imposed by the American defence has been cleverly bypassed by the scientists. Several tactical developments have pushed the accuracy level increasingly higher. Use of carrier wave in post-processing for increasing measurement resolution, dual frequency receiver to reduce ionospheric delays, differential mode to avoid S/A, use of precise ephemeries for better accuracy and use of better tropospheric models are few to name. This low cost, highly accurate and easy to use space geodetic technique is distinctly advantageous over the conventional terrestrial geodetic techniques like triangulation, trilateration and levelling. Unlike terrestrial surveys, GPS does not need line-of-sight clearance, measurement length is not limited by optical visibility and is much faster in operation.

GPS uses an earth-fixed earth-centred Cartesian coordinate system called World Geodetic System-84 (WGS-84), and gives coordinates of the measurement point in terms of X, Y and Z. Whereas these components can readily be converted in terms of latitude and longitude in any other system, height is given above a reference spheroid which has very little practical use. Conversion of this spheroidal height into orthometric (mean sea level) height, i.e. the height over geoid, requires knowledge about the geoid-spheroid separation, known as geoid undulation or geoid height at the measurement point. Geoid height of a single point on the surface can be actually measured by combined GPS and levelling measurements over the common point, or geoid undulation of a region can be modelled from gravity data. To test the viability of using GPS for height measurements, we carried out levelling and GPS surveys along a 100 km long profile in Ladakh of western Himalaya. The same geoid undulation was also computed from the global gravity model.

Spheroid is a mathematical, smooth surface, closest to the actual surface of the earth. Geoid is an equipotential gravity surface, a very close approximation to the mean sea level (msl), and is generally undulating depending on the local sub-surface mass distribution. As sea surface coincides with the geoid, it is much easier to map geoid undulations over the oceanic region. In fact, the